



LAWRENCE
LIVERMORE
NATIONAL
LABORATORY

Unification and extension of the similarity scaling criteria and mixing transition for studying astrophysics using high energy density laboratory experiments or numerical simulations

Y. Zhou

August 23, 2006

Plasma of Physics

Disclaimer

This document was prepared as an account of work sponsored by an agency of the United States Government. Neither the United States Government nor the University of California nor any of their employees, makes any warranty, express or implied, or assumes any legal liability or responsibility for the accuracy, completeness, or usefulness of any information, apparatus, product, or process disclosed, or represents that its use would not infringe privately owned rights. Reference herein to any specific commercial product, process, or service by trade name, trademark, manufacturer, or otherwise, does not necessarily constitute or imply its endorsement, recommendation, or favoring by the United States Government or the University of California. The views and opinions of authors expressed herein do not necessarily state or reflect those of the United States Government or the University of California, and shall not be used for advertising or product endorsement purposes.

Unification and extension of the similarity scaling criteria and mixing transition for studying astrophysics using high energy density laboratory experiments or numerical simulations

Ye Zhou
University of California
Lawrence Livermore National Laboratory, Livermore, CA 94550

The Euler similarity criteria for laboratory experiments and time-dependent mixing transition are important concepts introduced recently for application to prediction and analysis of astrophysical phenomena. However Euler scaling by itself provides no information on the distinctive spectral range of high Reynolds number turbulent flows found in astrophysics situations. On the other hand, time-dependent mixing transition gives no indication on whether a flow that just passed the mixing transition is sufficient to capture all of the significant dynamics of the complete astrophysical spectral range. In this paper, a new approach, based on additional insight gained from review of Navier-Stokes turbulence theory, is developed. It allows for revelations about the distinctive spectral scale dynamics associated with high Reynolds number astrophysical flows. From this perspective, we caution that the energy containing range of the turbulent flow measured in a laboratory setting must not be unintentionally contaminated in such a way that the interactive influences of this spectral scale range in the corresponding astrophysical situation cannot be faithfully represented. In this paper we introduce the concept of a *minimum state* as the lowest Reynolds number turbulent flow that a time-dependent mixing transition must achieve to fulfill this objective. Later in the paper we show that the Reynolds number of the *minimum state* may be determined as 1.6×10^5 . Our efforts here can be viewed as a unification and extension of the concepts of both similarity scaling and transient mixing transition concepts. At the last the implications of our approach in planning future intensive laser experiments or massively parallel numerical simulations are discussed. A systematic procedure is outlined so that as the capabilities of the laser interaction experiments and supporting results from detailed numerical simulations performed in recently advanced supercomputing facilities increase progressively, a strategy can be devised so that more and more spectral range dynamic structures and their statistical influences on evolving astrophysical flows can be progressively extended in laboratory investigations.

1. Introduction

In recent decades, improved instrumentation and advances in observational machinery and techniques have uncovered many new features and a revised picture of the incredibly rich complexity of evolutionary phenomena in extraterrestrial space [1-2]. At the same time, advances in laboratory scale experimental techniques such as use of modern high energy intensive pulsed laser beams have achieved capabilities which can produce energy densities in submillimeter-scale volumes that otherwise are only manifest in actual astrophysical events [see review by Remington *et al.*, references 2-3]. Beam target materials, pulse duration, energetic drive, etc. can be reproducibly prepared for generating conditions closely simulating scaled features of astrophysical events. These techniques are presently recreating aspects of astrophysical phenomena in the laboratory. This is tantamount to creation of experimental testbeds where theory and modeling can be quantitatively tested against astrophysical observations (so called *Laboratory Astrophysics*). In a laboratory setting, the initial conditions, diagnostic techniques, and energetic laser drives can be carefully controlled. A recent example was presented by Robey *et al.* [4] where an experimental testbed was designed using the Omega laser [5] for the study of the hydrodynamic issues of significance in studying supernovae [6-7]. It is anticipated that the much more powerful laser facilities currently under development such as the National Ignition Facility (NIF) [8-9] and French Laser Mégajoule (LMJ) [10-11], will provide enhanced opportunities for conducting much more advanced research in laboratory astrophysics [12].

As noted by Ryutov, Drake, and Remington, *et al.* [13], in the laboratory setting, the spatial and temporal scales are, roughly speaking, in the range of tens of micrometers and tens of nanoseconds. These scales are 10 to 20 orders of magnitude less than those of real astrophysical events (see Table 1, reproduced from data in Ref. [14]). From a hydrodynamic perspective, the turbulent flow and mixing in observed astrophysical events such as supernovae are associated with very high outer scale Reynolds numbers ($Re \sim 10^{10}$). Note here that the outer-scale Reynolds number Re is defined as $Re = \delta u / \nu$ [15]. Here u is the characteristic velocity, δ is the characteristic flow structure outer length scale, and ν is the kinematic viscosity.

In contrast, the typical Reynolds number that can be achieved in a laboratory experiment is $10^5 - 10^6$ [14]. Naturally, concern emerges as to whether this is of sufficient magnitude to investigate the physics of actual astrophysical events. In effect legitimate questions may be anticipated about the degree of confidence with which one can apply the laboratory results to interpretation of astrophysical phenomena [13].

Two recent efforts have been made in an attempt to address this question. First, Euler scaling has been proposed to relate the astrophysical problems to a laboratory experiment. For a system adequately described by the Euler equations, similarity criteria required for properly scaled experiments have been identified [13-14]. Second, in a high energy density physics (HEDP) experiment, the evolution of a turbulent mixing state always originates from accelerated (*i.e.* unsteady) development of flow instabilities. Corresponding to these accelerated conditions an unsteady turbulent mixing transition

criterion and a procedure for modeling and predicting the required time interval to achieve transition have been proposed [16-17]. This is an outgrowth and extension of the model analysis developed for stationary flows [18,19].

In this paper, we will first review these two recently developed concepts and point out the outstanding issues associated with them (Sec. 2). From the framework of general statistical Navier-Stokes turbulence theory one finds that the laboratory and astrophysical spectral ranges can and should be considered individually because of their significantly different interactive dynamics and influential spatial and temporal ranges. In this paper we introduce the concept of a “*minimum state*,” which is the turbulent flow state with the lowest Reynolds number in a laboratory setting that can faithfully reproduce the most significant (so called “energy containing”) scales of an astrophysics problem (Sec. 3). In Sec. 4, we will discuss the design requirements of the drive, timing, and diagnostic instruments (Sec. 5). The final section, Section 6, contains summary and conclusions.

2: Euler Scaling and Time-dependent Mixing Transition

A. Euler scaling

Similarity scaling is a familiar tool widely used to study issues physics generally but it may possess special emphasis in plasma physics [see for example, ref. 20]. Motivated in part by the general viewpoint of Zeldovich & Raizer [21] and Sedov [22], the Euler

similarity relationship [13] has been proven very helpful [2,4,12-14] in the development of laboratory astrophysics.

The Euler equation in conjunction with mass and energy conservation reads [23]

$$\begin{aligned}\rho \left[\frac{\partial u}{\partial t} + u \cdot \nabla u \right] &= -\nabla p \\ \frac{\partial \rho}{\partial t} + \nabla \cdot (\rho u) &= 0 \\ \frac{\partial p}{\partial t} - \gamma \frac{\partial \rho}{\partial t} + u \cdot \nabla p - \gamma \frac{p}{\rho} u \cdot \nabla \rho &= 0\end{aligned}$$

The first of these equations is the momentum balance equation, the second is the continuity equation, and the third representing the conservation of energy appears here in the form of an entropy conservation equation for a polytropic gas. Ryutov *et al.* [13] noted that under the scaling transformation

$$\begin{aligned}r_{astro} &= \tilde{r} \ r_{lab}, \quad u_{astro} = \tilde{u} \ u_{lab}, \quad \rho_{astro} = \tilde{\rho} \ \rho_{lab}, \\ t_{astro} &= t_{lab} \frac{\tilde{r}}{\tilde{u}}, \quad p_{astro} = p_{lab} \ \tilde{p} = p_{lab} \ \tilde{\rho} \tilde{u}^2\end{aligned}$$

the Euler equation remains invariant, as long as the following Euler number is preserved

$$\tilde{p} = \tilde{\rho} \tilde{u}^2.$$

The Euler equations, while generally useful for laboratory scaling, are limited by neglect of viscosity (Ryutov and Remington [24] were aware of this issue and have suggested several novel experiments to help resolve the sensitivity). This limitation to Euler scaling can be traced back to the fact that significant physical viscous features such as growth and dissipation of vorticity only develop when the full Navier-Stokes equation is applied.

Of particular interest here, Euler scaling does not provide information on the specific size range of statistical dynamic flow structures that can be scaled accurately.

The distinctive spectral scales are a hallmark of high Reynolds number turbulent flows. From the theoretical turbulence (Navier-Stokes) perspective, the presence of strong nonlinear interactions creates a profoundly complex multiple scale dynamic problem for investigation. The reader is referred to Fig. 1, which is a nearly comprehensive superposition of energy spectra compiled from a large variety of wind-tunnel and geophysical flows [25]. The challenge is to account for all the statistical scales of motion, starting from the largest (lowest wave number) where the energy injection occurs to the smallest, the Kolmogorov dissipation scale [26], where viscous energy dissipation acts as an absolute limit to the macroscopic scales of motion. (The Kolmogorov scale is given by, $\lambda_K = (\nu^3/\epsilon)^{1/4}$, where ν is the kinematic viscosity and ϵ is the dissipation rate [15,26]). The low wave number energy injection scale limit is where external forcing acts to drive the system. The evolution of the energy containing scales governs the overall development of the flow field [15,26]. With less than Navier Stokes generality as a basis, Euler scaling is not able to reveal the physical influences of these distinctive spectral ranges.

B. Time-dependent mixing transition

Many experiments have been conducted in classical fluid dynamics facilities, shock tubes, and laser facilities (such as the Omega laser) to understand the complex

phenomena. Due to diagnostic limitations typical measurements consist solely of the growth of the mixing zone width. While these widths (of the bubble and spike fronts, individually or combined) are usually measured, it is difficult to know whether or not a particular experiment has reached mixing transition. (It should be noted that the analysis of time-dependent mixing transition is applicable to any flow. However, the published examples [16-17] were specialized to the Rayleigh-Taylor [27-29] and Richtmyer-Meshkov [30-31] flows). This type of information cannot be easily obtained from flow visualization [17].

The mixing transition concept for *stationary* fluid flows, developed at Caltech [18,19], refers to the transition to a turbulent state in which the flow drives rapid mixing at the molecular scale. This turbulent state leads to rapid dissipation of momentum and of concentration fluctuations (mixing). The classical Kolmogorov theory [26] assumes the existence of an inertial range, where the dynamics are isolated within an intermediate scale range, λ , which cannot be influenced by the outer, low frequency scales, δ , where turbulent energy is produced, nor can it be influenced by the inner, high frequency, viscous dissipation scales

$$\lambda_K \ll \lambda \ll \delta.$$

Dimotakis [19] proposed that the extent of the effective inertial range could be narrowed to

$$\lambda_K < \lambda_v \ll \lambda \ll \lambda_{L-T} < \delta,$$

Here the lower-limit of the inertial range is the inner viscous scale $\lambda_v = 50\lambda_K$, where the Kolmogorov microscale can be rewritten as $\lambda_K = \delta \text{Re}^{-3/4}$. The upper-limit of the

inertial range is the Liepmann-Taylor scale $\lambda_{L-T} = 5\lambda_T$, where $\lambda_T = \delta \text{Re}^{-1/2}$ is the well known Taylor correlation microscale [26].

We have extended the stationary mixing transition to time-dependent flows and applied it to a wide range of experiments [16-17]. The Liepmann-Taylor scale essentially describes the internal laminar vorticity growth layer generated by viscous shear along the boundaries of a large-scale feature of size δ . The temporal development of such a laminar viscous layer is well known to go as $(\nu t)^{1/2}$ (Stokes [32], Rayleigh [27], Lamb [33]).

$$\lambda_D = C (\nu t)^{1/2}$$

Hence, the upper bound of the developing inertial range is the smaller of the Liepmann-Taylor scale, λ_{L-T} and λ_D . Here the coefficient of the diffusion layer, C , was suggested as $C \approx \sqrt{15}$ both for isotropic, homogeneous turbulence [34] and for steady parallel flows, and as $C \equiv 5$ [35] for laminar boundary layer flows (following the Liepmann-Taylor constant by Dimotakis [19]).

The inertial range is presumed to be established when the evolution of the large-scale, $\min\{\lambda_D, \lambda_{L-T}\}$, is decoupled from the inner viscous scale, λ_ν . For time-dependent flows, the mixing transition is achieved when a range of scales exists such that the temporally evolving upper bound $[\min\{\lambda_D, \lambda_{L-T}\}]$ is significantly larger than the temporally evolving lower bound, λ_ν . Thus, the mixing transition occurs if and when the inequality [16-17]

$$\min\{\lambda_{L-T}(t), \lambda_D(t)\} > \lambda_v(t) \equiv 50\lambda_k(t)$$

is satisfied.

In designing and interpreting experiments for time-dependent flows, the time-dependent mixing transition provided the desirable ability to estimate the time required to achieve the mixing transition state. However, one may ask, is a flow that has just passed the mixing transition enough to capture all the physics of energy-containing scales?

If not, how high must the Reynolds number be?

3. The *Minimum State*

As indicated in Table 1 (data from Remington and Ryutov [14]), the astrophysics problems of interest (Supernova was used as an example in the table), have extremely high Reynolds numbers. From an application perspective, accurate description of the time-dependent, three-dimensional evolution of the energy-containing scales may be all that is needed. Therefore, it is important to capture these scales accurately (all relevant length scales are summarized in Table 2 for the convenience of the reader [36]).

The determination of the Reynolds number for the *minimum state* is based on detailed studies on energy transfer associated with interacting scales [references 37-41]. The limit to the reach of a wavenumber k where it may directly interact is with the mode that is twice the size of its own value. (All more distantly separated interactions decay too rapidly for influence as evidenced by the $-4/3$ scaling drop off of *disparity parameter* vs.

energy flux in the inertial range [37-38,42]). Recall that the highest wave number (smallest length scale) of the energy containing scales ($k' \subseteq [0, k_{L-T}]$) is k_{L-T} , beyond which appears the beginning of the inertial range. To prevent the energy containing scales from being contaminated by the dissipation scales demands that a critical wavenumber, hereafter denoted $k_Z \equiv 2 k_{L-T}$, be located in the inertial range.

The *minimum state* is defined as the turbulent flow which has the *lowest* Reynolds number that captures the energy containing scales of the astrophysics problems in a laboratory or simulation setting. The *minimum state* is therefore the lowest Reynolds number turbulent flow where all the modes in the energy containing scales ($k' \subseteq [0, k_{L-T}^*]$) will only interact with modes in the same spectral range or those within the inertial range ($[0, k_{L-T}^*] \cup (k_{L-T}^*, k_v^*]$). Obviously, this requirement is introduced to take full advantage of the universality of the inertial range.

The *minimum state*, according to this definition, is the turbulent flow that takes the value of k_Z equal to the inner-viscous wavenumber (the end of the inertial range): $k_Z^* \equiv 2 k_{L-T}^* = k_v^*$ (see Fig. 2). Using the definition of k_{L-T} and k_v , one finds that the *critical* Reynolds number of the *minimum state* is $Re^* = 1.6 \times 10^5$.

Note that the outer-scale Reynolds number is approximately related to the Taylor microscale Reynolds number by $R_\lambda = (20/3)^{1/2} Re^{1/2}$ in isotropic flow [34] and $R_\lambda \approx 1.4 Re^{1/2}$ for turbulence in the far field of a jet [43,44]. As a result, the

corresponding *critical* Taylor-microscale Reynolds number of the *minimum state* is $(1.4-2.58) \times Re^{1/2}$ ($R_\lambda^* \approx 560-1033$).

The *minimum state* is the baseline turbulent state that any laboratory astrophysics experiments (or computations using astrophysical simulations codes) must be achieved. This requirement is needed in order to faithfully reproduce the interactive dynamics and their influences on the energy containing scales of the original astrophysical situation. The dynamics of this most important spectral scale [26] can be scaled down from an extremely high Re astrophysical turbulent flow to a high, but manageable Re flow in either laboratory experiment or a simulation setting.

Recall once again that the inertial range is bounded between the Liepmann-Taylor scale and the inner-viscous wavenumber, $[k_{L-T}, k_v]$. For a turbulent flow in the *minimum state*, the inertial range of the astrophysics phenomenon will not be reproduced accurately in a laboratory setting. The reason is that modes of the inertial range of the *minimum state* may interact directly with those in the dissipation scales. The dissipation scale in a turbulent flow is not universal and depends on the Reynolds number [45,41]. As a result, the inertial range modes will be contaminated in the *minimum state*.

After establishing the significance of the *minimum state* in the laboratory astrophysics, the experiments (or simulations) should achieve Re^* or higher. The *first* implication of our analysis is that the intensity or the timing of the drive or the materials must be adjusted for achieving or surpassing this goal.

4. The similarity scaling based on Navier-Stokes turbulence

At this point, it is necessary to introduce the resolution cutoff of the diagnostics (denoted as λ_C in physical space or k_C in wavenumber). In this section, for the sake of brevity, the cutoff wavenumber is chosen to be the same as the Liepmann-Taylor wavenumber, namely $k_C = k_{L-T}$. In next section, a more general situation will be discussed and the desired requirement for the diagnostic resolution will be determined as $k_C \geq k_{L-T}$. The rational for this choice will be given in some detail in next section.

The Navier-Stokes equation can now be divided into the resolvable ($k \leq k_C$) and subgrid scales ($k > k_C$). For obvious reason, the new similarity scaling will be constructed for the resolvable scale only ($k \leq k_C$). The resolvable scale Navier-Stokes equation can be written as

$$\frac{\partial \rho u^<}{\partial t} + \nabla \bullet (\rho [u^< u^< + 2 u^< u^> + u^> u^>]) + \nabla p^< = \mu \nabla^2 u^<$$

where $u^<$ and $u^>$ denote the resolvable and subgrid scale velocity fields, respectively.

The parameter μ is the dynamic viscosity [46] and for simplicity in this example the flow is assumed either incompressible or weakly compressible.

The energy transfer resulted from the distant interactions, $u^>u^>$, has been shown to behave in the same fashion as that of the molecular viscosity [47]. The subgrid-subgrid interactions can be therefore satisfactorily modeled as eddy viscosity, $\mu(r)$ (or $\mu(k)$ in wavenumber space). The resolvable Navier-Stokes equation can then be written as

$$\frac{\partial \rho u^<}{\partial t} + \nabla \bullet (\rho [u^<u^< + 2 u^<u^>]) + \nabla p^< = \mu(r) \nabla^2 u^<$$

For the cutoff wavenumber k_C (as long as it is in an inertial range, $k_C \geq k_{L-T}$), the statistic turbulence closure theories lead [47-49] to

$$\nu(r) = \mu(r) / \rho \propto \epsilon^{1/3} r^{4/3}$$

We now take further advantage of the observation that the flows of interest are essentially incompressible. The Mach number of a RT induced turbulent flow [27-29] is restricted to a very low value [50]. Also, the RM induced turbulence flow [30-31] can be viewed as a freely decaying incompressible flow [51-52].

The resolvable scale Navier-Stokes equation now is ready for a scale similarity analysis. From the astrophysics to the lab framework, the scaling transformation is given by

$$t_{astro} = t_{lab} \tilde{r} / \tilde{u}, \quad p_{astro} = p_{lab} \tilde{p} = p_{lab} \tilde{\rho} \tilde{u}^2$$

$$r_{astro} = \tilde{r} \ r_{lab}, \quad u_{astro} = \tilde{u} \ u_{lab}, \quad \rho_{astro} = \tilde{\rho} \ \rho_{lab},$$

$$\nu(k)_{astro} = \nu(k)_{lab} \tilde{\nu} = \nu_{lab} \tilde{r} \tilde{u}$$

The scaled Navier-Stokes equation in the laboratory framework is

$$\frac{\partial \mathbf{u}_{lab}^{<}}{\partial t} + \nabla_{lab} \bullet \left(\rho [\mathbf{u}_{lab}^{<} \mathbf{u}_{lab}^{<} + 2 \mathbf{u}_{lab}^{<} \mathbf{u}_{lab}^{>}] \right) + \nabla_{lab} p_{lab} = \nu_{lab}(r) \nabla_{lab}^2 \mathbf{u}_{lab}^{<}$$

and remains an invariant in relation to that of the original form for the astrophysics setting.

5. Resolution requirement, scale up, and statistical subgrid modeling

A. Resolution requirement:

For the sake of brevity, we have so far restricted ourselves to the simple case where the diagnostic cutoff wavenumber of the resolution, k_C takes the same value as that of the boundary between the energy-containing and inertial ranges, the Liepmann-Taylor wavenumber, k_{L-T} . For a given Reynolds number there are three situations that one may encounter (for all relevant length scales, see Table 2) in an experiment. These different scenarios will depend on the limitations to the refinement of the diagnostics resolution used for the experiment. Specifically, different situations arise based on whether all of the energy containing scales, $[0, k_C]$, can be resolved by the instrumentation. The simplest one is the one we have already employed in last section, $k_C = k_{L-T}$. Another possibility is the undesirable situation where not all the modes in the energy containing

scale ($k_C < k_{L-T}$) will be resolved. This clearly undesirable possibility need not be considered further here.

The last possibility is when the resolution is excessively fine, for example when $k_C > k_{L-T}$. While generally additional refinement in the resolution may seem desirable, one should note that it is not necessary to refine the resolution over the value of $(1/2)k_v$. This limit on the resolution refinement is firm for any given flow field, since beyond that, the resolved scale range will include contaminated modes that have interacted directly with the dissipation scale.

This subsection leads to the *second* implication of our analysis to the experimental design, now in terms of the diagnostic instrumentation. Once the Reynolds number of an experiment is determined, the requirement for resolving the range of contained scales or some greater range will immediately inform the experimentalist of the resolution required (for an illustrative example, see Table 3).

B. A recipe for planning an experiment:

For the convenience of the reader, the implications of the theoretical analysis for planning a HEDP experiment to achieve the Reynolds number at the *minimum state* or beyond is summarized below.

Step 1. Choose the materials and drive carefully to achieve the minimum state or beyond ($Re \geq Re^*=1.6 \times 10^5$).

The viscosity is evaluated, the outer scale or the characteristic velocity is computed, and the Reynolds number is determined.

Step 2. Design the diagnostics to insure that the resolvable scale or beyond can be captured.

Several other useful parameters are next determined (see table 2), including the Liepmann-Taylor wavenumber, k_{L-T} the inner viscous wavenumber, k_v , and the critical wavenumber of the minimum state, $k_Z = 2k_{L-T}$. The highest wavenumber that needs to be resolved is $k_v/2$.

Step 3. Post experiment data analysis.

The captured domain from the experiment can be subdivided into two parts: $\Delta k_E = [0, k_{L-T}]$ represents the energy containing scales and $\Delta k_I = [k_{L-T}, k_Z]$ represents the inertial range scales ($k_Z \leq k_v/2$, note again that the resolution does not need to extend beyond $k_v/2$). The corresponding spectral scales of astrophysical flow situations under study can be determined using the scaling transformation.

C. Plan of future experiments: scale up in Re

The scaling analysis in this paper does offer suggestions for planning future HEDP experiments. It is reasonable to expect that the capabilities of future experiments will advance progressively with increased intensity of drives and increased sophistication of the diagnostics capabilities.

Let the very first experiment (serving as the baseline) be denoted experiment 0. Denote the subsequent experiments representing future increasing facility capability as experiments $\{1, 2, \dots, N\}$. In turn, the values of the experimental Reynolds number and diagnostic resolution refinement may be denoted:

$$\{Re^0, Re^1, \dots, Re^{N-1}, Re^N\} \quad \text{and} \quad \{k_C^0, k_C^1, \dots, k_C^{N-1}, k_C^N\}$$

where $Re^0 < Re^1 < \dots < Re^{N-1} < Re^N$ and $k_C^0 > k_C^1 > \dots > k_C^{N-1} > k_C^N$.

A sequence of succeeding experiments can be utilized to increase the spectral range of an astrophysical situation that can be reproduced in the laboratory. The baseline experiment, introduced previously in last subsection, is established as an experiment to achieve the Reynolds number of the minimum state or beyond $Re^0 \geq Re^*$. The second requirement is that the cutoff of the resolution resolves all the energy containing scales. The baseline experiment, of course, captures at the energy containing scale where $Re^0 = Re^*$. In the case of $Re^0 \geq Re^*$, a fraction of the inertial range may also be captured.

This process can be repeated with incremental increases in resolution as the values of the Reynolds numbers become higher and higher. At the same time, more and more spectral scales (specifically, larger and larger fraction of the inertial range) will be captured in the experiment facility since the resolution cutoff wavenumber also becomes higher and higher. Therefore, incrementally more spectral information attending an astrophysical event can be reproduced in the laboratory environments as the development and refinement of the facilities proceed.

D. Small scale statistics modeling:

While the subgrid scales cannot be measured directly, some statistical properties of the inertial range are available from statistical turbulence closure theories [53]. Essentially, the fundamental building block of the energy transfer, the triadic interaction function, $T(k,p,q)$, follows the self-similarity relationship [53,37-38]

$$T(k,p,q) = a^3 T(ak,ap,aq),$$

for three dimensional turbulence. This scaling works well as long as all six wavenumber are located in the inertial range (This requirement is met here since the cutoff wavenumber of the resolution, k_C takes the value $k_C > k_{L-T}$).

The triadic interaction transfer function is a relationship that will provide all the statistical information in an inertial range. Since the energy in the inertial range is transferred from

the energy containing scale, a matching condition is needed to complete the subgrid modeling procedure.

According to Kolmogorov [26], the energy flux (ϵ) is the only link that connects the energy containing scale to the universal inertial ranges. The energy flux is given by [26]

$$\epsilon = D_\epsilon \tilde{u}^3 / \delta,$$

where D_ϵ is a constant and \tilde{u} is the characteristic velocity of the energy containing eddies [26,54-59].

The overall level of the triadic interaction function can now be set. Note that [15,26]

$$\epsilon = \int T(k) dk$$

Here $T(k) \equiv \sum_{\{p,q\}} T(k,p,q)$

and $T(k,p,q)$ is the triadic interaction function [37-38, 41] (wavenumbers k,p,q all in the inertial range).

It is useful to note that the statistical information can also be recovered for a high Re two-dimensional flow. A corresponding interaction relationship also exists for two dimensional turbulent flows [53]. For two dimensional situations a parallel procedure can be trivially developed and applied but further elaboration is not considered justified in this paper. .

6. Summary and conclusions

In this paper, we have considered two concepts that are highly relevant to laboratory astrophysics: the Euler similarity scaling between astrophysics problem and laboratory experiment and the time-dependent mixing transition. The limitations of these concepts are discussed in order to illustrate where progress is urgently needed. Specifically, with Euler scaling alone, we are unable to give consideration to the distinctive spectral range of high Reynolds number turbulent flows characteristic of astrophysical events under study.. On the other hand the recently developed time-dependent mixing transition criterion by itself gives no indication as to whether a flow that just passed the mixing transition is sufficient to capture all the physics of the important spectral range. A new framework, based on Navier-Stokes statistical turbulence flow theory, has been developed that unifies and extends these two concepts. The distinctive spectral scales, the characteristics of high Reynolds number astrophysical turbulent flows, may now be considered. A *minimum state* is introduced as the lowest Reynolds number turbulent state in a laboratory or computation setting that insures that the energy containing scales are not contaminated by the dissipation scales. The *minimum state* also provides the lowest Reynolds that a laboratory experiment or a numerical simulation of time-dependent flow must achieve. This critical Reynolds number is found to be 1.6×10^5 , an order of magnitude higher than the Reynolds number that corresponds to transient mixing transition. At the same time, as long as the Reynolds number of a flow has passed this critical Reynolds number, the energy containing scale of an astrophysical event can be faithfully reproduced. Finally, the high energy density intense pulsed laser facilities.

supercomputer platforms, and diagnostics instrumentation and techniques can be expected to progressively improve in successive stages over time. A strategy is needed and has been offered in detail so that an experimentalist may be able to systematically adapt advances in high intensity lasers, measurements, and refined diagnostic analyses to recover more distinctive information on spectral spatial structure and statistical details influencing the evolution of astrophysical events.

ACKNOWLEDGMENTS

The author is very grateful to Dr. Alfred C. Buckingham for his critical reading and suggestions. He also thanks Prof. Dale Pullin for brining Ref. 18 to his attention. This work was performed under the auspices of the U.S. Department of Energy by the University of California, Lawrence Livermore National Laboratory under Contract No. W-7405-Eng-48.

Reference:

1. R.P. Drake, *J. Geophys. Res.*, **104**, 14505 (1999);
R.P. Drake, “HED facilities and their connection to issues in astrophysics,”
presented at *Sixth International High Energy Density Astrophysics Conference*,
Houston, TX (March, 2006); available online at <http://www.hedla.org/>.
2. B. A. Remington, R. P. Drake, and D. D. Ryutov, *Rev. Mod. Phys.*, **78**, 755
(2006)
3. B.A. Remington, D. Arnett, R.P. Drake, and H. Takabe, *Science*, **284**, 1488
(1999);
B.A. Remington, R.P. Drake, H. Takabe, and D. Arnett, *Phys. Plasma*, **7**, 1641
(2000)
4. H.F. Robey, J.O. Kane, B.A. Remington *et al.*, *Phys. Plasma*, **8**, 2446 (2001)
5. J.M. Soures, R.L. McCrory, C.P. Verdon *et al.* *Phys. Plasma*, **3**, 2108 (1996)
6. E. Muller, B. Fryxell, and D. Arnett, *Astron. Astrophys.* **564**, 896 (1991)
7. K. Kifonidis, T. Plewa, H.-Th. Janka, and E. Muller, *Astrophys. J. Lett*, **531**, L123
(2000)
8. W.J. Hogan *et al.*, *Nucl. Fusion*, **41**, 567 (2001)
9. G.H. Miller, E.I. Moses, and C.R. Wuest, *Nucl. Fusion*, **44**, S228 (2004)
10. M.L. Andre, *Fusion Eng. Des.*, **44**, 43 (2001)
11. J. Tassart, *Nucl. Fusion*, **44**, S134 (2004)
12. B.A. Remington, *Plasma Phys. Control. Fusion*, **47**, A191 (2005);
13. D.D. Ryutov, R.P. Drake, J. Kane, E. Liang, B.A. Remington, and W.M. Wood-
Vasey, *Astrophys. J.*, **518**, 821 (1999);
D.D. Ryutov, R.P. Drake, and B.A. Remington, *Astrophys. J. Supp*, **127**, 465
(2000)
14. D.D. Ryutov and B.A. Remington, *Plasma Phys. Control. Fusion*, **44**, B407
(2002)

15. J.O. Hinze, *Turbulence*, 2nd ed, (McGraw Hill, New York, 1975);
A.S. Monin and A.M. Yaglom, *Statistical Fluid Mechanics*, (MIT Press, Cambridge, MA 1975)
16. Y. Zhou, H.F. Robey, and A.C. Buckingham, *Phys. Rev. E*, **67**, 056305 (2003);
Y. Zhou, B.A. Remington, H.F. Robey et al. *Phys. Plasma*, **10**, 1883 (2003)
17. H.F. Robey, Y. Zhou, A.C. Buckingham et al. *Phys. Plasma*, **10**, 614 (2003)
18. A. Roshko, *AIAA Journal*, **14**, 1349 (1976);
J. Konrad and A. Roshko, *Bull. American Physical Society*, **21**, 1229, (1976)
19. P.E. Dimotakis, *J. Fluid Mech.*, **409**, 69 (2000)
20. J.W. Connor and J.B. Taylor, *Nuclear Fusion*, **17**, 5 (1977);
M. Murakami and S. Iida, *Phys. Plasma*, **9**, 2745 (2002)
21. Y.B. Zeldovich & Y.P. Raiser, *Physics of Shock Waves and High-Temperature Hydrodynamic Phenomena* (Academic, New York, 1966)
22. L.I. Sedov, *Mechanics of Continuous Media* (World Scientific, Singapore, 1997)
23. L.D. Landau and E.M. Lifshitz, *Fluid Mechanics*, (Pergamon, Oxford, 1987)
24. D.D. Ryutov and B.A. Remington, *Phys. Plasma*, **10**, 2629 (2003)
25. S.G. Saddoughi and S.V. Veeravalli, *J. Fluid Mech.*, **268**, 333 (1994)
26. G. K. Batchelor, *Theory of Homogeneous Turbulence*, (Cambridge University Press, Cambridge, 1953).
27. Lord Rayleigh, *Proc. Roy. Math. Soc.*, **14**, 170 (1883);
28. Lord Rayleigh, *Phil. Mag.* **6**, **xxi**, 697, (1911);
29. G.I. Taylor, *Proc. R. Soc. London, Ser A*, **201**, 192 (1950)
30. R.D. Richtmyer, *Comm. Pure Appl. Math*, **13**, 297 (2001);
31. E.E. Meshkov, *Izv. Akad. Sci., USSR Fluid Dyn.*, **4**, 101 (1969)

32. G.G. Stokes, *Trans. Cambr. Phil. Soc.* 9, Part II. 8-106. (Reprinted): (1901):
Math. & Phys. Papers, 3, Cambr. Univ. Press, London and New York. 1-141.
33. H. Lamb, *Hydrodynamics*, (Cambridge Univ. Press, London, 1932).
34. H. Tennekes and J.L. Lumley, *First Course in Turbulence* (MIT Press, Cambridge, MA, 1972)
35. H. Schlichting, *Boundary-Layer Theory*, (McGraw-Hill, New York, 1951)
36. The discussion can proceed in both physical and spectral spaces. The spectral representation is used more extensively in this and next sections for describing the spectral scales and triadic interactions
37. Y. Zhou, *Phys. Fluids A*, **5**, 1092 (1993);
38. Y. Zhou, *Phys. Fluids A*, **5**, 2511 (1993)
39. J.A. Domaradzki and E.M. Saiki, *Phys. Fluids*, **9**, 2148 (1997);
J.A. Domaradzki and K.-C. Loh, *Phys. Fluids*, **11**, 2330 (1999);
J.A. Domaradzki and N.A. Adams, *J. of Turbulence*, **3**, 024, pp. 1, (2002).
40. T. Dubois, F. Jauberteau, and Y. Zhou, *Physica D*, **100**, 390, (1997)
41. Y. Zhou and C.G. Speziale, *Appl. Mech. Rev.*, **51**, 267 (1998)
42. T. Gotoh and T. Watanabe, *J. Turbulence*, **6**, 33 p. 1 (2005)
43. D.R. Dowling and P.E. Dimotakis, *J. Fluid Mech.*, **218**, 109 (1990)
44. P.L. Miller and P.E. Dimotakis, *Phys. Fluids A*, **3**, 1156 (1990)
45. D. Martinez, S. Chen. G. Doolen, R.H. Kraichnan, L.P. Wang and Y. Zhou
J. Plasma Phys., **57**, 195 (1997)
46. R.B. Bird, W.E. Stewart, and E.N. Lightfoot, *Transport Phenomena*, (Wiley, New York, 1960)

- 47. Y. Zhou and G. Vahala, *Phys. Rev. E*, **47**, 2503 (1993)
- 48. R.H. Kraichnan, *Phys. Fluids*, **30**, 1583 (1987)
- 49. Y. Zhou, G. Vahala, and M. Hossain, *Phys. Rev. A.*, Vol. **40**, 5865, (1989)
- 50. J.P. Mellado, S. Sarkar, and Y. Zhou, *Phys. Fluids*, **17**, 076101 (2005)
- 51. Y. Zhou, *Phys. Fluids*, **13**, 538 (2001);
T.T. Clark and Y. Zhou, *J. Applied Mech.*, **73**, 461 (2006)
- 52. Y. Zhou, R. Rubinstein, D. Eliason, W. Cabot, *Astron. Astrophys.*, **405**, 379 (2003)
- 53. R.H. Kraichnan, *J. Fluid Mech.*, **47**, 525 (1971)
- 54. K.R. Sreenivasan, *Phys. Fluids*, **27**, 1048, (1984)
- 55. K.R. Sreenivasan, *Phys. Fluids*, **10**, 528 (1998).
- 56. P.K. Yeung and Y. Zhou, *Phys. Rev. E*, **56**, 1746 (1997)
- 57. B.R. Pearson, P.-A. Krogstad, and W. van de Water, *Phys. Fluids*, **14**, 1288, (2002).
- 58. Y. Keneda, T. Ishihara, M. Yokokawa, K. Itakura, and A. Uno, *Phys. Fluids*, **15**, L21, (2003)
- 59. P. Burattini, P. Lavole, and R.A. Antonia, *Phys. Fluids*, **17**, 098103, 1 (2005).

Parameters	SN1987a	Laboratory experiments
r (cm)	9×10^{10}	5.3×10^{-3}
u (cm/s)	2×10^7	1.3×10^5
ρ (g/cm³)	7.5×10^{-3}	4.2
<i>Eu</i>	0.29	0.34
<i>Re</i>	2.6×10^{10}	1.7×10^6

Table 1. Comparing parameters of a SN1987a plasma in the He-H transition layer and parameters of the laboratory experiment. Data from Table 1 of Ryutov and Remington (ref. 14)

Length scale	δ	λ_η	λ_{L-T}	λ_ν	λ_z	λ_c
Wave-number ($2\pi/\text{length}$)	k_δ	k_η	k_{L-T}	k_ν	k_z	k_c
<p>Note and remarks</p> <p>(The remarks on this row will be based on the physical length scales)</p>	The outer scale. The largest scale of the flow	The Kolmogorov length scale. The viscous interaction dominates at smallest length scales	The Liepmann-Taylor length scale. This is the upper bound of the inertial range. This length scale separates the energy containing and inertial ranges. Note that the minimum state requires that the energy containing scale, $[\lambda_{L-T}, \delta]$, is resolved	<p>The inner-viscous length scale. This is the lower boundary of the inertial range. This length scale separates the inertial and dissipation ranges.</p> <p>Note that $2\lambda_\nu$ is the finest length scale needed for diagnostics</p>	<p>The smallest physical scale beyond which the energy containing scale will not interact directly. It is defined as $(\lambda_{L-T}/2)$.</p> <p>Our theory demands it resides within the inertial range</p>	The length scale that separates the resolvable and subgrid scales. This is the smallest physical length scale that the diagnostic instruments can resolve

Table 2. nomenclature of all relevant length scales

Re	δ (cm)	λ_v (cm)	λ_{L-T} (cm)	λ_z (cm) ($\lambda_z = 0.5\lambda_{L-T}$)
1.7×10^6	5.3×10^{-3}	5.6×10^{-6}	2.0×10^{-5}	1.0×10^{-5}

Table 3. The length scale values for the typical laboratory experiment in Table 1 (data taken from Ryutov and Remington, 2002, ref. 14). The outer length scale is 5.3×10^{-3} cm and the outer scale Reynolds number is 1.7×10^6 . The upper (Liepmann-Taylor) and lower (inner-viscous) boundaries of the inertial range are 2.0×10^{-5} cm and 5.6×10^{-6} cm, respectively. The energy containing scale of this experiment will not interact with the physical length scales with their values smaller than λ_z , which has the value of 1.0×10^{-5} cm.

Energy containing scales, external forcing

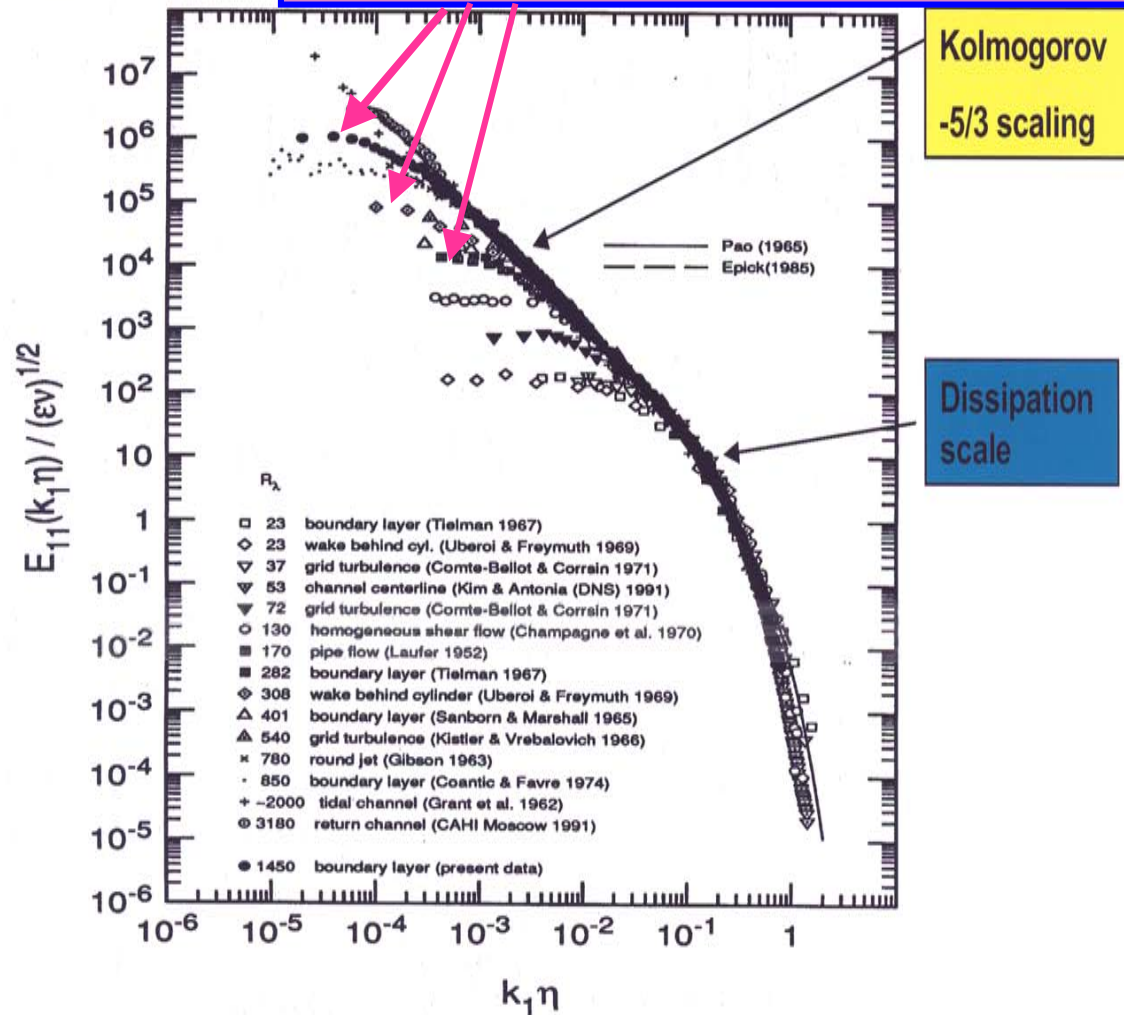


Fig. 1. Distinctive spectral scales from a large collection of the wind-tunnel and geophysical experiments (reproduced from Ref. 25). The values of the Reynolds numbers here are based on the Taylor microscale [refs. 15 and 26]. The compensated longitudinal energy spectra is plotted against the longitudinal wave number, which is normalized by the Kolmogorov length scale. Note that there are very strong Reynolds number dependences in the dissipation spectral scales. For these flows with high Reynolds numbers, there are extended inertial ranges which may exist over several decades. The energy containing scales, of course, are different from flow to flow because of the different external driving forces.

Fig. 2. The illustration of the minimum state. This is the turbulent flow that has the lowest Laboratory-Astrophysical representative Reynolds number, but with sufficiently extended inertial range to insure that the energy containing scale will not be unintentionally contaminated by the dissipation scale. The Reynolds number of the minimum state, a universal value, may be determined as 1.6×10^5 . This is can be obtained by requiring that $K_v = K_z = 2 K_{L-T}$

